

# Gas-phase study of the reactivity of optical coating materials with hydrocarbons by use of a desktop-size extreme-ultraviolet laser

Scott Heinbuch,<sup>1,2,\*</sup> Feng Dong,<sup>2,3</sup> Jorge J. Rocca,<sup>1,2</sup> and Elliot R. Bernstein<sup>2,3</sup>

<sup>1</sup>*Department of Electrical and Computer Engineering, Colorado State University, 1320 Campus Delivery, Fort Collins, Colorado 80523-1320, USA*

<sup>2</sup>*National Science Foundation, Engineering Research Center for Extreme Ultraviolet Science and Technology, Colorado State University, 1320 Campus Delivery, Fort Collins, Colorado 80523-1320, USA*

<sup>3</sup>*Department of Chemistry, Colorado State University, 1872 Campus Delivery, Fort Collins, Colorado 80523-1872, USA*

\*Corresponding author: shein@engr.colostate.edu

Received December 11, 2007; revised March 12, 2008; accepted March 21, 2008;  
posted April 3, 2008 (Doc. ID 90662); published May 21, 2008

The reactivity of prospective capping-layer extreme-ultraviolet (EUV) mirror materials with hydrocarbons is studied in the gas phase by use of mass spectroscopy of metal-oxide clusters. We report the results of chemistry studies for  $\text{Si}_m$ ,  $\text{Ti}_m$ ,  $\text{Hf}_m$ , and  $\text{Zr}_m\text{O}_n$  metal-oxide clusters in which the reaction products were ionized with little or no fragmentation by 26.5 eV photons from a desktop-size 46.9 nm Ne-like Ar laser. Hf and Zr oxides are found to be much less reactive than Si or Ti oxides in the presence of EUV light. The results are relevant to the design of EUV mirror capping layers that are resistant to carbon contamination. © 2008 Optical Society of America

OCIS codes: 140.7240, 160.4670, 160.4760, 300.6170, 310.6860, 340.7480.

## 1. INTRODUCTION

The implementation of extreme-ultraviolet (EUV) lithography as a manufacturing tool for the fabrication of future generations of computer chips requires a solution to the problem of the degradation of the reflectivity of EUV mirrors and masks caused by carbon deposition in the presence of EUV light. This motivates the study of the reaction of prospective metal-oxide capping-layer materials with hydrocarbons. An increased understanding of these reactions could lead to the development of thin capping layers that might protect EUV optics from carbon buildup. Metal-oxide nanoparticles are widely used in chemical reactions for industrial processes, and as of yet, there is not a proper understanding of these chemical reaction processes due to complicated environments on condensed phase surfaces. Clusters provide a path to the elucidation of chemical activity under isolated, controlled, and reproducible conditions through a detailed mechanistic model for condensed phase and surface reactivity and reactions.

In general, two primary reactive threats contribute to a loss of EUV mirror reflectivity: (1) growth of a carbonaceous layer on the mirror surface caused by the EUV-induced dissociation of adsorbed hydrocarbons and (2) oxidation of the mirror surface by the radiative dissociation of adsorbed water [1–4]. Whether an optic is oxidized or carbonized in a given environment depends in part on the relative amounts of  $\text{H}_2\text{O}$  and hydrocarbon in the gas-phase environment. The surface chemistry is currently not well understood. A better understanding could result

from studies of clusters in the gas phase, where the clusters can serve as general models for multilayer mirror coatings under ideal reproducible conditions.

Silicon is a material that is widely used as the top layer in multilayer EUV optics that easily oxidizes on the surface leading to the growth of oxide layers upon EUV radiation [2–4] (see Fig. 1). During the oxidation process, adsorbed water molecules are dissociated by secondary electrons from the incident EUV radiation and the oxygen atoms react with the Si surface to create  $\text{SiO}_2$  [5–7]. This is considered to be an irreversible process causing reflection loss. However, Meiling *et al.* [3] have shown that the oxidation process can be slowed by up to a factor of 6 by using smart gas blends during exposure, such as ethanol. Similarly, carbon contamination occurs when EUV-induced photoelectrons crack hydrocarbon molecules that are adsorbed on the mirror surface causing reflection loss [4,8,9]. Meiling *et al.* [3] found that carbon growth can be suppressed by a factor of up to 50 by admitting  $\text{O}_2$  into the vacuum system during exposure. Carbon contamination is a reversible process in which adding  $\text{O}_2$  to the system increases time between cleanings of the optics [2,10].

To reduce these reflection loss processes, researchers are searching for materials that are robust to oxidation and carbon deposition in the presence of EUV light and that will extend multilayer mirror lifetimes using capping layers consisting of, but not limited to, materials such as SiC, SiN, Pt, Ru, Pd, and Rh [11]. Of these materials, ruthenium has emerged as the most promising [12]. Reportedly, a 5 nm Ru capping layer on a Si surface can increase

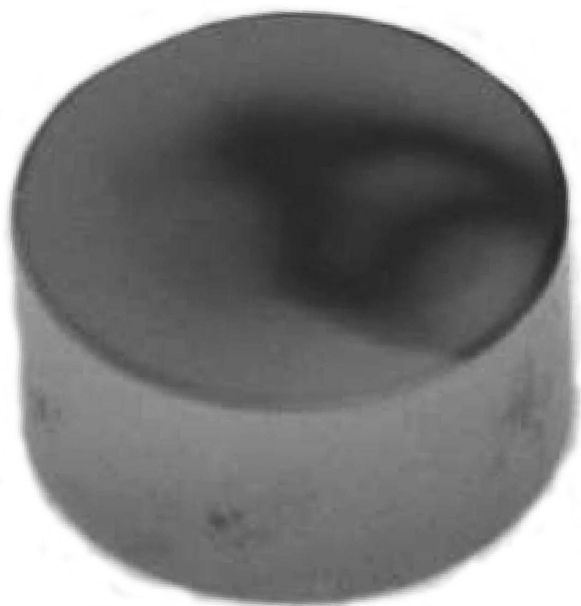


Fig. 1. Photograph of a Sc/Si multilayer mirror that has been exposed to 46.9 nm radiation from a capillary discharge laser for  $\sim 500$  h. Carbon deposit has contaminated a large portion of the mirror, greatly reducing its reflectivity.

mirror lifetime by a factor of  $\sim 40$  while exhibiting minimal reflection loss of the MoSi multilayer structure [11]. Nonetheless, while Ru reduces oxidation effects, it does not show the same promise in the reduction of carbon contamination. Other potential candidates to protect the reactive Si surface are thin coatings of titanium/hafnium/zirconium oxide to help reduce the effect of hydrocarbon growth. This report will focus on the reactivity of  $\text{Si}_m\text{O}_n$ ,  $\text{Ti}_m\text{O}_n$ ,  $\text{Hf}_m\text{O}_n$ , and  $\text{Zr}_m\text{O}_n$  clusters in the gas phase. The conclusions drawn from these studies can help elucidate reactions on optical surfaces.

We have recently completed a series of studies that constitute the first demonstration of the use of EUV lasers in photophysics and photochemistry [13–18]. These studies have primarily focused on finding active catalysts for the improvement of industrial processes. The experiments were based on the use of a compact capillary discharge EUV laser in the study of clusters and cluster reactions. The EUV laser was used to provide single-photon ionization of the neutral clusters for mass spectroscopy studies, with the significant advantage of reduced cluster fragmentation with respect to multiphoton or electron ionization sources. In the present study, we are searching for materials that are not active, in the presence of common vacuum system contaminants (e.g., water, carbon oxides, nitrogen oxides, hydrocarbons) and EUV light, in the process of oxidation of carbon deposition on optical surfaces. For this purpose, Si/Ti/Hf/Zr oxide neutral clusters are generated in a conventional laser vaporization/supersonic expansion cluster source by laser ablation of the appropriate metal wafer/foil into a He carrier gas mixed with 5%  $\text{O}_2$  at 80 psi (gauge). Neutral clusters pass through a reactor cell into which a reaction gas is input by a pulsed valve. Single-photon ionization of the neutral clusters and reaction products takes place using a 46.9 nm (26.5 eV)

laser [19,20] in the ionization region of a time-of-flight mass spectrometer (TOFMS). The capillary discharge EUV laser emits pulses of  $\sim 1.5$  ns duration with an energy/pulse of  $\sim 10$   $\mu\text{J}$  at a repetition rate of up to 12 Hz [19,20]. A time-of-flight (linear/reflectron) mass spectrometer is employed for mass analysis.

The experiments were carried out in a flow tube reactor that is similar to the one adopted by Geusic *et al.* [21] (Fig. 2). A short summary of our flow tube experimental equipment is given below.

$\text{M}_m\text{O}_n$  ( $\text{M}=\text{Si}, \text{Ti}, \text{Hf}, \text{or Zr}$ ) clusters are generated by laser ablation with a focused 532 nm laser ( $\text{Nd}^{3+}:\text{YAG}$ , 10 Hz, 5–8  $\text{mJ}/\text{cm}^2$ , 8 ns duration) onto a 12 mm diameter spring-loaded metal disk in the presence of a pulsed helium carrier gas mixed with 5%  $\text{O}_2$ , controlled by a R.M. Jordan supersonic nozzle. A translational and rotational (spiral) motion of the disk is managed by a single motor (Maxon) that is powered by a homemade controller with a wide range of speed adjustments. Metal-oxide clusters are formed in an adjustable length gas channel with a waiting room upstream. Typical dimensions used in this system are 3 mm diameter by 5 mm length for the waiting room and 1.8 mm diameter by 44 mm length for the rest of the channel. The gas channel is directly coupled to a tube/reactor (stainless steel, 6.3 mm inner diameter by 76 mm length). The reactant gases,  $\text{C}_2\text{H}_2$ ,  $\text{C}_2\text{H}_4$ , water, etc., are injected into the reactor by a second pulsed valve (General Valve, Series 9) with a pulse duration of  $\sim 1$  ms. The delay time between the two valve openings is optimized to yield the best product signals. Pressure in the flow tube reactor is estimated to be  $\sim 1$  Torr in the presence of a reactant gas pulse. After reaction of  $\text{M}_m\text{O}_n$  with hydrocarbons, or other constituents in the reactor, reactants, products, and the buffer gases are expanded into vacuum (ca.  $2 \times 10^{-7}$  Torr) to form a molecular beam. The beam enters the detection region of a mass spectrometer chamber (ca.  $10^{-6}$ – $10^{-7}$  Torr) through a 4 mm diameter skimmer. The clusters and products in the beam are ionized by a 46.9 nm EUV laser that is described in detail in the literature via [19,20].

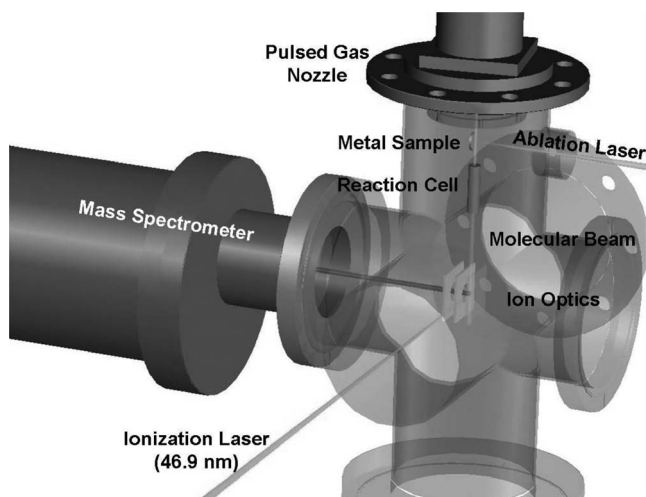


Fig. 2. Schematic representation of the TOFMS experiment.  $\text{M}_m\text{O}_n$  metal-oxide clusters are generated by 532 nm laser ablation of a metal target and the clusters are passed through a reaction cell. The products, reactants, and buffer gases are ionized by a 46.9 nm laser and detected by TOFMS.

The EUV laser pulse energy is  $\sim 10 \mu\text{J}$  at the output of the laser but is reduced to  $\sim 3\text{--}5 \mu\text{J}$  at the output of a z-fold mirror system placed just before the ionization region with the purpose of providing alignment capability of the beam with respect to the cluster setup. The z-fold consists of two gold-coated mirrors at grazing incidence: a toroidal mirror with a 50 cm focal length that focuses the incoming beam, and a planar mirror that directs the beam into the ionization region. The cluster ions produced are perpendicularly extracted to the molecular beam and enter the 1.0 m long flight tube in which they are separated in arrival time according to their mass. At the end of the flight tube, the ions are reflected back down the flight tube by reflector plates, refocused, and detected by a microchannel plate (MCP) detector operating with a pulsed bias voltage in order to gate large He signals and prevent saturation of the detector. Signals from the detector are fed to a digital oscilloscope through a  $50 \Omega$  miniature high voltage (MHV) connector. Time delays between the pulsed valve opening, firing the ablation laser, injecting the reaction gas, firing the ionization laser, and gating the MCPs are generated by three programmable digital delay generators. All timings can be adjusted to maximize the spectral signal strength.

In conventional cluster spectroscopy systems that make use of visible or UV wavelength laser photoionization, multiphoton absorptions cause fragmentation of the clusters (left side of Fig. 3). During the multiphoton ionization process by a nanosecond light pulse, at least two processes can be responsible for cluster ionization: (1) a cluster can absorb a photon through low-lying electronic states and relax back to the ground electronic state many times, thus heating the cluster until thermionic emission occurs, and (2) vertical absorption of two or more photons can occur without rapid relaxation between absorption steps for both neutral and ionic species. In either case, fragmentation of the cluster is likely [22]. The EUV laser source drastically changes the ionization process (right side of Fig. 3) so that multiphoton effects are eliminated. For example, SiO has an ionization energy of  $\sim 11.5$  eV. Ionization using an ArF excimer laser at 193 nm (6.4 eV) requires multiple photons, whereas ionization at 46.9 nm (26.5 eV) has more than enough photon energy to ionize SiO with a single photon. The photoelectron carries away the remaining excess energy above the vertical ionization energy, resulting in almost no fragmentation of the clusters [13–18] and neutral parent cluster information is retained.

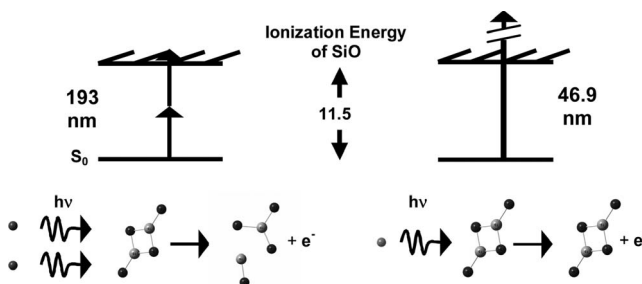


Fig. 3. Left, multiphoton ionization fragment molecules. Right, 26.5 eV photons from compact Ne-like Ar EUV laser allows single-photon ionization of any cluster or molecule with little or no fragmentation.

The high energy per pulse ( $\sim 10 \mu\text{J}$ ) and the repetition rate of several hertz of the capillary discharge 46.9 nm laser developed for this purpose is well matched with the repetition rate of the cluster source that utilizes a commercial 10 Hz Nd:YAG laser for sample ablation. The EUV laser is especially important for the study of metal-oxide clusters because it ionizes the clusters by single-photon transitions and thereby prevents subsequent cluster fragmentation and loss of parent cluster mass information.

## 2. RESULTS

Water and hydrocarbon contaminants are a major problem in EUV optic environments because they are extremely difficult to remove even in high-vacuum enclosures and they readily adsorb onto surfaces. Secondary electrons generated by the incident EUV flux, and to a lesser extent the EUV radiation itself, dissociate the water and hydrocarbons and are believed to contaminate optics surfaces [23].

### A. Silicon Oxide Cluster ( $\text{Si}_m\text{O}_n$ ) Reactions

Figure 4 depicts mass spectra of the  $\text{Si}_m\text{O}_n$  cluster distribution with no reactant present [Fig. 4(a)] and reaction products with water [ $\text{H}_2\text{O}$ —Fig. 4(b)], acetylene

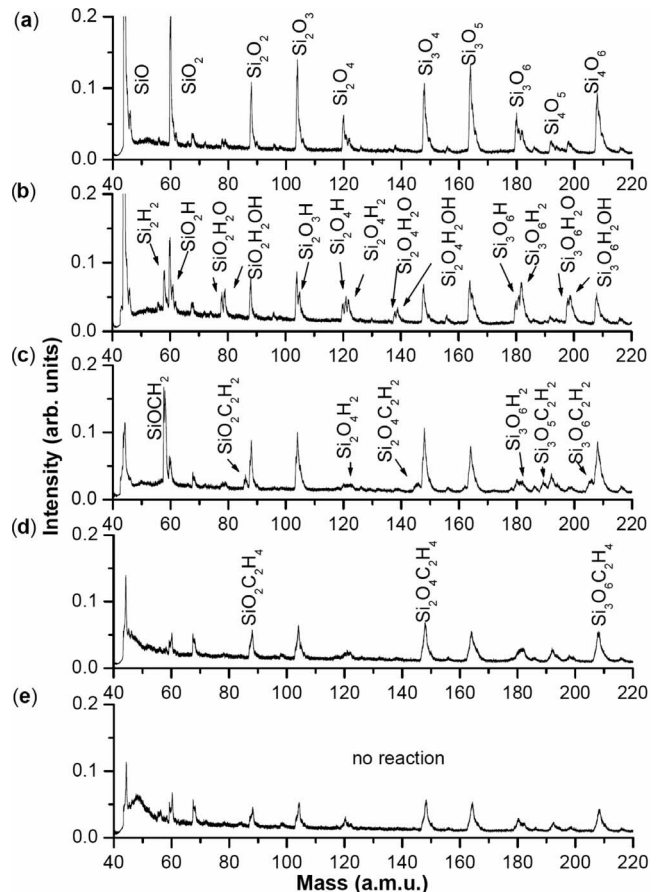


Fig. 4.  $\text{Si}_m\text{O}_n$  cluster distribution (a) with no reactant in the reaction cell, (b) with water in the reaction cell, (c) with acetylene ( $\text{C}_2\text{H}_2$ ) in the reaction cell, (d) with ethylene ( $\text{C}_2\text{H}_4$ ) in the reaction cell, and (e) with ethane ( $\text{C}_2\text{H}_6$ ) in the reaction cell.

[C<sub>2</sub>H<sub>2</sub>—Fig. 4(c)], ethylene [C<sub>2</sub>H<sub>4</sub>—Fig. 4(d)], and ethane [C<sub>2</sub>H<sub>6</sub>—Fig. 4(e)]. In Fig. 4(a), the cluster distribution, with no reactant, is dominated by oxygen-deficient clusters, such as Si<sub>2</sub>O<sub>2,3</sub> and Si<sub>3</sub>O<sub>4,5</sub>. No oxygen-rich clusters such as Si<sub>2</sub>O<sub>5</sub> or Si<sub>3</sub>O<sub>7</sub> are observed. These respective clusters are labeled oxygen rich or deficient because the most stable cluster configuration is of the nature (SiO<sub>2</sub>)<sub>n</sub>, for example, Si<sub>2</sub>O<sub>4</sub> and Si<sub>3</sub>O<sub>6</sub>. Silicon-oxide clusters tend to lose one or more oxygen atoms upon EUV radiation.

To study neutral Si<sub>m</sub>O<sub>n</sub> cluster reactions with water, the reactant is pulsed into the reactor in its vapor phase. When the neutral clusters generated from the ablation/expansion source pass through the reactor cell, collisions will occur between neutral Si<sub>m</sub>O<sub>n</sub> clusters and the water. A new distribution of neutral clusters and reaction products is obtained by using 26.5 eV laser ionization. As shown in Fig. 4(b), when water is added to the reactor, products from the reaction Si<sub>m</sub>O<sub>n</sub>+H<sub>2</sub>O are generated through an association channel,



forming products SiO<sub>2</sub>H<sub>2</sub>O, Si<sub>2</sub>O<sub>4</sub>H<sub>2</sub>O, and Si<sub>3</sub>O<sub>6</sub>H<sub>2</sub>O. Generally, the most stable silicon clusters of the form (SiO<sub>2</sub>)<sub>n</sub> are more active with water than oxygen-deficient clusters are. The most stable silicon-oxide clusters are also observed to take hydrogen atoms from water to form SiO<sub>2</sub>H, Si<sub>2</sub>O<sub>4</sub>H<sub>1,2</sub>, and Si<sub>3</sub>O<sub>6</sub>H<sub>1,2</sub> through reaction channels



Hydrocarbons are also commonly present in vacuum enclosures, largely originating from the enclosed system components (e.g., photoresist, outgassing products) and these are similarly adsorbed and dissociated [23]. To study neutral Si<sub>m</sub>O<sub>n</sub> cluster reactions with hydrocarbons, the reactants acetylene (C<sub>2</sub>H<sub>2</sub>), ethylene (C<sub>2</sub>H<sub>4</sub>), and ethane (C<sub>2</sub>H<sub>6</sub>) gases are individually and separately pulsed into the reactor consequently causing collisions between neutral Si<sub>m</sub>O<sub>n</sub> clusters and the reactants.

When C<sub>2</sub>H<sub>2</sub> gas is added to the reactor, many new product signals, formed in the reaction of Si<sub>m</sub>O<sub>n</sub>+C<sub>2</sub>H<sub>2</sub>, are observed in the mass spectra, as shown in Fig. 4(c). The major products, SiO<sub>2</sub>C<sub>2</sub>H<sub>2</sub>, Si<sub>2</sub>O<sub>4</sub>C<sub>2</sub>H<sub>2</sub>, Si<sub>3</sub>O<sub>6</sub>C<sub>2</sub>H<sub>2</sub>, etc., are generated from the association reactions



Additionally, new products, SiOCH<sub>2</sub>, Si<sub>2</sub>O<sub>4</sub>H<sub>2</sub>, and Si<sub>3</sub>O<sub>6</sub>H<sub>2</sub>, are found. In general, the most stable silicon-oxide clusters are more active with acetylene than oxygen-deficient clusters are.

As shown in Fig. 4(d), the major products of the reaction Si<sub>m</sub>O<sub>n</sub>+C<sub>2</sub>H<sub>4</sub> are assigned as SiO<sub>2</sub>C<sub>2</sub>H<sub>4</sub>, Si<sub>2</sub>O<sub>4</sub>C<sub>2</sub>H<sub>4</sub>, and Si<sub>3</sub>O<sub>6</sub>C<sub>2</sub>H<sub>4</sub> generated from an association reaction channel,

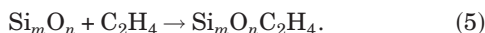


Figure 4(e) illustrates that all cluster signals decrease in roughly the same proportion when the saturated hydrocarbon C<sub>2</sub>H<sub>6</sub> gas is added to the reactor cell. A similar

result is also observed when inert gases are added to the reactor cell. Therefore, the decrease of cluster signals is due to scattering by the C<sub>2</sub>H<sub>6</sub> gas pulsed into the reactor. No major reaction channel is observed.

The reactivity of Si<sub>m</sub>O<sub>n</sub> clusters is not solely limited to water and these three hydrocarbon species. In fact, we find that Si<sub>m</sub>O<sub>n</sub> clusters are highly reactive with many unsaturated hydrocarbons, formic acid, and alcohols, suggesting that the oxidized Si surface in the condensed phase will easily be contaminated by these and a number of other reactants.

## B. Titanium Oxide Cluster (Ti<sub>m</sub>O<sub>n</sub>) Reactions

The photocatalytic activity of titanium oxide results in thin coatings of the material exhibiting self-cleaning and self-disinfecting properties under exposure to UV radiation [24]. These properties make the material a candidate for applications, such as protective capping layers on EUV mirrors.

The reactivity of titanium oxide clusters is explored in the gas phase and an example is shown in Fig. 5 that depicts mass spectra of the Ti<sub>m</sub>O<sub>n</sub> cluster distribution [Fig. 5(a)] and reaction products with H<sub>2</sub>O [Fig. 5(b)], C<sub>2</sub>H<sub>2</sub> [Fig. 5(c)], C<sub>2</sub>H<sub>4</sub> [Fig. 5(d)], and C<sub>2</sub>H<sub>6</sub> [Fig. 5(e)]. The cluster distribution is once again dominated by oxygen-

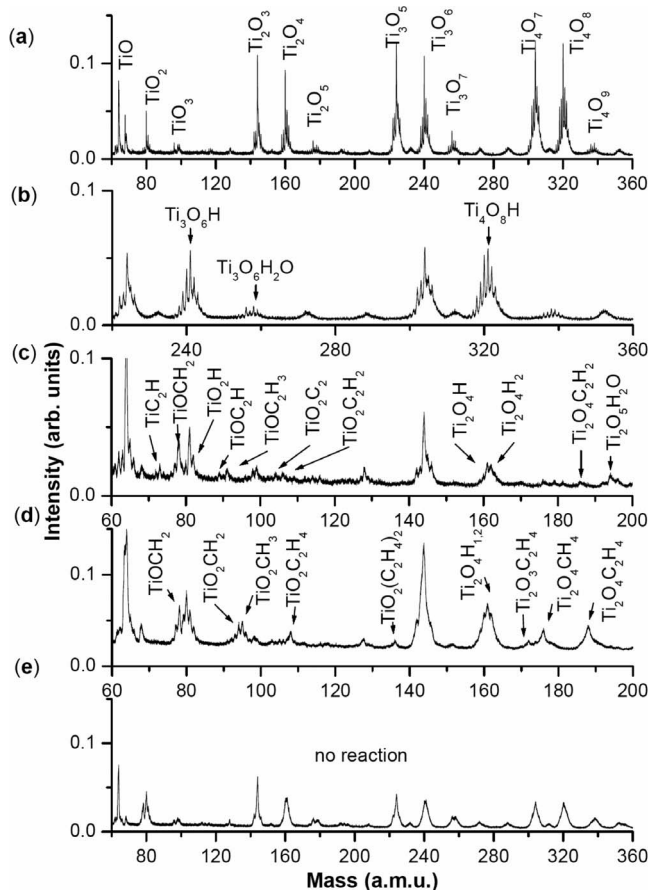


Fig. 5. (Note that the scales on each section are different in order to better display the data.) Ti<sub>m</sub>O<sub>n</sub> cluster distribution (a) with no reactant in the reaction cell, (b) with water in the reaction cell, (c) with acetylene (C<sub>2</sub>H<sub>2</sub>) in the reaction cell, (d) with ethylene (C<sub>2</sub>H<sub>4</sub>) in the reaction cell, and (e) with ethane (C<sub>2</sub>H<sub>6</sub>) in the reaction cell.

deficient clusters, such as  $\text{TiO}$  and  $\text{Ti}_2\text{O}_3$ . Contrary to the  $\text{Si}_m\text{O}_n$  cluster distribution, oxygen-rich clusters, such as  $\text{TiO}_3$  and  $\text{Ti}_2\text{O}_5$  are observed although the signals are weak. Also, the mass resolution of our experimental setup allows us to observe the isotopic structure of the  $\text{Ti}_m\text{O}_n$  clusters.

To study neutral  $\text{Ti}_m\text{O}_n$  cluster reactions with water or hydrocarbons, the experimental method is exactly the same as for  $\text{Si}_m\text{O}_n$  cluster reactions where the reactant gases are individually and separately pulsed into the reactor. As shown in Fig. 5(b), when water is added to the reactor, products from the reaction  $\text{Ti}_m\text{O}_n + \text{H}_2\text{O}$  are generated through an association channel to form  $\text{Ti}_3\text{O}_4\text{H}_2\text{O}$ , and products where  $\text{Ti}_m\text{O}_n$  clusters take H atoms from water to form  $\text{Ti}_3\text{O}_4\text{H}$  and  $\text{Ti}_4\text{O}_8\text{H}$  are generated.

When acetylene gas is added to the reactor, many new product signals, formed in the reaction of  $\text{Ti}_m\text{O}_n + \text{C}_2\text{H}_2$ , are observed in the mass spectra, as shown in Fig. 5(c). Generally, the most stable titanium clusters of the form  $(\text{TiO}_2)_n$  are more active with acetylene than oxygen-deficient clusters are, generating association products, such as  $\text{TiO}_2\text{C}_2\text{H}_2$  and  $\text{Ti}_2\text{O}_4\text{C}_2\text{H}_2$ . However, some reactions occur involving oxygen-deficient clusters to form  $\text{TiOCH}_2$ ,  $\text{TiOC}_2\text{H}$ , and  $\text{TiOC}_2\text{H}_2$ . Additionally, oxygen-stable and oxygen-rich clusters generate new products,  $\text{TiO}_2\text{H}$ ,  $\text{TiO}_2\text{C}_2$ ,  $\text{Ti}_2\text{O}_4\text{H}_{1,2}$ , and  $\text{Ti}_2\text{O}_6\text{H}_2$ .

When ethylene is added to the reactor, we observe association products generated from  $\text{Ti}_m\text{O}_n + \text{C}_2\text{H}_4$  [Fig. 5(d)]. Generally, the most stable titanium clusters of the form  $(\text{TiO}_2)_n$  are more active with ethylene than oxygen-deficient clusters, generating products, such as  $\text{TiO}_2\text{C}_2\text{H}_{2,3,4}$  and  $\text{Ti}_2\text{O}_4\text{C}_2\text{H}_4$ . A few reactions involving oxygen-deficient clusters are also observed to generate  $\text{TiOCH}_2$  and  $\text{Ti}_2\text{O}_3\text{C}_2\text{H}_4$ . The most stable titanium clusters are also observed to take hydrogen atoms from ethylene and break apart ethylene to form products, such as  $\text{TiO}_2\text{CH}_2$ ,  $\text{TiO}_2\text{CH}_3$ , and  $\text{Ti}_2\text{O}_4\text{H}_{1,2}$ .

Figure 5(e) illustrates that all the cluster signals decrease in roughly the same proportion when the saturated hydrocarbon  $\text{C}_2\text{H}_6$  gas is added to the reactor cell. Again, the decreased cluster signal is due to scattering by the  $\text{C}_2\text{H}_6$  gas pulsed into the reactor. No major reaction channel is observed.

In a similar fashion to  $\text{Si}_m\text{O}_n$  metal-oxide clusters, the reactivity of  $\text{Ti}_m\text{O}_n$  metal-oxide clusters is not limited in any way to any one reactant. We find that  $\text{Ti}_m\text{O}_n$  clusters are highly reactive with many unsaturated hydrocarbons, formic acid, water, and alcohols, suggesting that the oxidized Ti surface is similar to the oxidized Si surface and in the condensed phase will also easily be contaminated by these reactants.

### C. Hafnium-Oxide Cluster ( $\text{Hf}_m\text{O}_n$ ) Reactions

$\text{HfO}_2$  is characterized by good chemical, thermal, and mechanical stability that facilitates its use even under severe conditions [25], making it another good candidate for a protective capping layer. The reactivity of hafnium-oxide clusters is explored in the gas phase and an example is shown in Fig. 6, which depicts mass spectra of the  $\text{Hf}_m\text{O}_n$  cluster distribution [Fig. 6(a)] and reaction products with  $\text{H}_2\text{O}$  [Fig. 6(b)],  $\text{C}_2\text{H}_2$  [Fig. 6(c)],  $\text{C}_2\text{H}_4$  [Fig. 6(d)], and  $\text{C}_2\text{H}_6$  [Fig. 6(e)]. The cluster distribution domi-

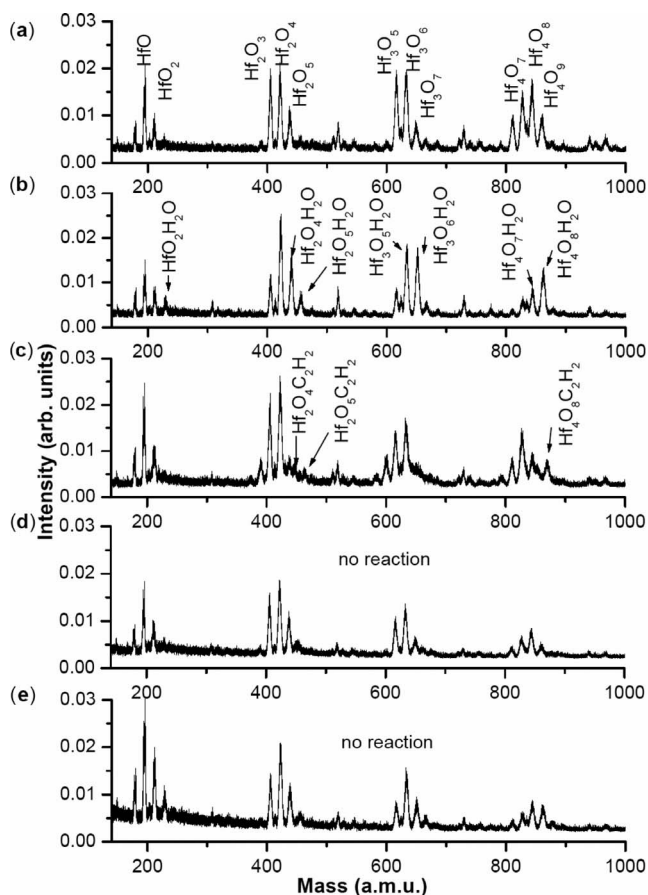


Fig. 6.  $\text{Hf}_m\text{O}_n$  cluster distribution (a) with no reactant in the reaction cell, (b) with water in the reaction cell, (c) with acetylene ( $\text{C}_2\text{H}_2$ ) in the reaction cell, (d) with ethylene ( $\text{C}_2\text{H}_4$ ) in the reaction cell, and (e) with ethane ( $\text{C}_2\text{H}_6$ ) in the reaction cell.

nance is shared by both oxygen-deficient and oxygen-stable clusters of the type  $(\text{Hf}_n\text{O}_{2n-1})_n$  and  $(\text{HfO}_2)_m$ , respectively. Oxygen-rich clusters,  $(\text{Hf}_n\text{O}_{2n+1})_n$ , are observed although the signals are smaller than the oxygen-deficient and oxygen-stable clusters.

The experimental method is exactly the same as for  $\text{Si}_m/\text{Ti}_m\text{O}_n$  cluster reactions, in which case the reactant gases are individually and separately pulsed into the reactor. As shown in Fig. 6(b), when water is added to the reactor, products from the reaction  $\text{Hf}_m\text{O}_n + \text{H}_2\text{O}$  are generated through an association channel,



Only association reactions involving oxygen-stable and oxygen-rich clusters are observed for  $\text{Hf}_m\text{O}_n + \text{H}_2\text{O}$ .

When acetylene gas is added to the reactor, very few new product signals, formed in the reaction of  $\text{Hf}_m\text{O}_n + \text{C}_2\text{H}_2$ , are observed in the mass spectra, as shown in Fig. 6(c). Only the most stable hafnium clusters and oxygen-rich hafnium clusters are active with acetylene, generating association products, such as  $\text{Hf}_2\text{O}_4\text{C}_2\text{H}_2$ ,  $\text{Hf}_2\text{O}_5\text{C}_2\text{H}_2$ , and  $\text{Hf}_4\text{O}_8\text{C}_2\text{H}_2$ . No reactions occur involving oxygen-deficient clusters.

When ethylene or ethane, shown in Figs. 6(d) and 6(e), respectively, are added to the reactor, the cluster signals decrease in roughly the same proportion as when inert

gases are added to the reactor cell. Therefore, the decrease of cluster signals is due to scattering by the  $C_2H_4$  and  $C_2H_6$  gas pulsed into the reactor in the presence of  $Hf_mO_n$  clusters. No major reaction channel is observed.

In contrast to the behavior of  $Si_mO_n$  and  $Ti_mO_n$  metal-oxide clusters, the reactivity of  $Hf_mO_n$  metal-oxide clusters is limited to a few reactants. We find that  $Hf_mO_n$  clusters are highly unreactive with many unsaturated hydrocarbons and alcohols. Even when  $Hf_mO_n$  clusters react, the reaction products are few and only involve oxygen-stable and oxygen-rich structures through association channels. No significant chemistry is observed. These data suggest that the oxidized Hf surface is less reactive than the oxidized Si and Ti surfaces and in the condensed phase will be contaminated to a much lesser extent by these reactants.

#### D. Zirconium-Oxide Cluster ( $Zr_mO_n$ ) Reactions

$ZrO_2$  is characterized by extreme thermal, chemical, and mechanical stability, which gives rise to a wide range of technical applications for  $ZrO_2$  thin films and coatings, especially in optics [26] and protective applications [27], making the material a candidate for protective capping layers on EUV mirrors.

The reactivity of zirconium oxide clusters is explored in the gas phase and an example is shown in Fig. 7, which

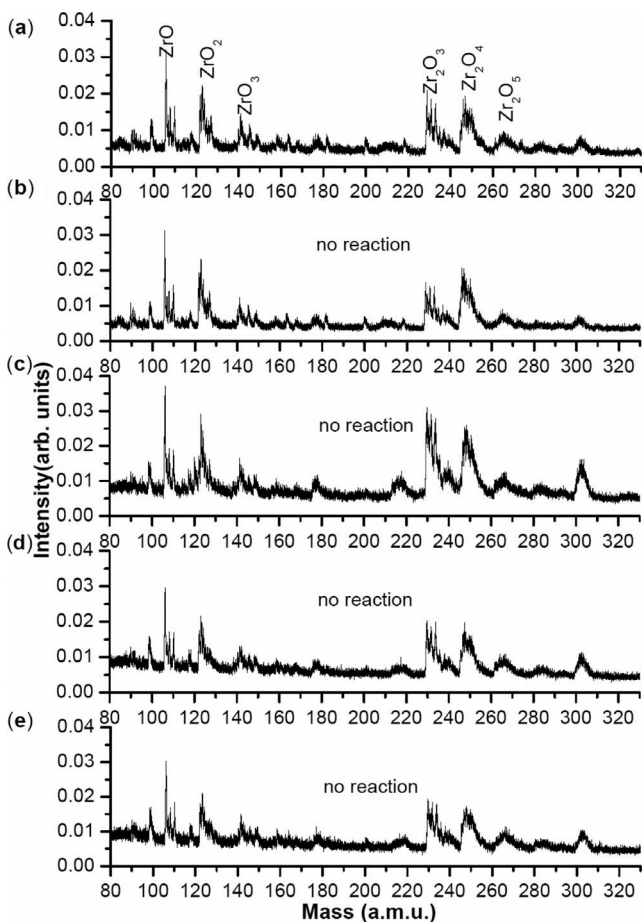


Fig. 7.  $Zr_mO_n$  cluster distribution (a) with no reactant in the reaction cell, (b) with water in the reaction cell, (c) with acetylene ( $C_2H_2$ ) in the reaction cell, (d) with ethylene ( $C_2H_4$ ) in the reaction cell, and (e) with ethane ( $C_2H_6$ ) in the reaction cell.

depicts mass spectra of the  $Zr_mO_n$  cluster distribution [Fig. 7(a)] and reaction products with  $H_2O$  [Fig. 7(b)],  $C_2H_2$  [Fig. 7(c)],  $C_2H_4$  [Fig. 7(d)], and  $C_2H_6$  [Fig. 7(e)]. The cluster distribution dominance, much like  $Hf_mO_n$ , is shared by both oxygen-deficient and oxygen-stable clusters of the types  $(Zr_nO_{2n-1})_n$  and  $(ZrO_2)_n$ , respectively. Oxygen-rich clusters,  $(Zr_nO_{2n+1})_n$ , are observed although the signals are smaller than the oxygen-deficient and oxygen-stable clusters.

The experimental method is the same as for  $Si_m/Ti_m/Hf_mO_n$  cluster reactions in which case the reactant gases are individually and separately pulsed into the reactor. We find that  $Zr_mO_n$  clusters are highly unreactive with any reactant that we introduce into the system. These data suggest that the oxidized  $Zr_mO_n$  surface is less reactive than the oxidized Si, Ti, and even Hf oxide surfaces. The results suggest that a zirconium oxide film will be contaminated to a much lesser extent by these reactants.

### 3. CONCLUSIONS

In general, two primary reactive threats contribute to a loss of EUV mirror reflectivity: (1) the growth of a carbonaceous layer on the mirror surface caused by the EUV-induced dissociation of adsorbed hydrocarbons and (2) the oxidation of the mirror surface by the radiative dissociation of adsorbed water. We have studied four different materials in the gas phase with the intention of relating our data and observations to the application of protective coatings for EUV mirror surfaces. Silicon mirror surfaces are readily oxidized and contaminated upon EUV irradiation [2–4]. Our spectra involving  $Si_mO_n$  metal-oxide clusters and their reactions with many unsaturated hydrocarbons, water, and alcohols, show that  $Si_mO_n$  clusters are reactive in the gas phase. This suggests that an oxidized Si surface in the condensed phase will be highly reactive. Titanium-oxide photocatalytic activity has demonstrated thin coatings of the material exhibiting self-cleaning and self-disinfecting properties under exposure to UV radiation that would be desirable for protecting EUV optic surfaces. Nonetheless, our spectra involving  $Ti_mO_n$  metal-oxide clusters and their reaction with many unsaturated hydrocarbons, water, and alcohols show that  $Ti_mO_n$  clusters are reactive in the gas phase. The data show that silicon- and titanium-oxide capping layers in optical coatings may be easily contaminated by residual gases in vacuum and should be avoided and protected in the presence of EUV irradiation.

Conversely, our spectra involving zirconium and hafnium metal-oxide clusters and their reaction with many unsaturated hydrocarbons, water, and alcohols show that they are unreactive in the gas phase. These data suggest that oxidized hafnium and zirconium surfaces in the condensed phase are much less reactive than Ti or Si oxide surfaces. Zirconium oxide is less reactive than hafnium oxide. Hf and Zr oxides should make good protective coatings for EUV optical surfaces and extend optical lifetimes upon EUV irradiation.

Also, it is observed that oxygen-deficient clusters in all four cases are less reactive than oxygen-rich and oxygen-stable clusters. This result suggests that if a surface is

tailored to be oxygen poor, this condition could also help protect an EUV optic surface from carbon contamination and help increase the lifetime of EUV optics.

Currently, we are undergoing studies that involve the contamination of  $\text{Si}_m/\text{Ti}_m/\text{Hf}_m/\text{Zr}_m\text{O}_n$  surfaces in the condensed phase. Preliminary results parallel the cluster studies presented in this paper, but further work is required to arrive at definitive conclusions.

## ACKNOWLEDGMENTS

This work was supported by the National Science Foundation (NSF), Engineering Research Center for Extreme Ultraviolet Science and Technology under NSF award 0310717, Philip Morris, USA, and the US Department of Energy, Basic Energy Sciences program.

## REFERENCES

- J. Hollenshead and L. Klebanoff, "Modeling extreme ultraviolet/ $\text{H}_2\text{O}$  oxidation of ruthenium optic coatings," *J. Vac. Sci. Technol. B* **24**, 118–130 (2006).
- B. Mertens, M. Weiss, H. Meiling, R. Klein, E. Louis, R. Kurt, M. Wedowski, H. Trenkler, B. Wolschrijn, R. Jansen, A. Runstraat, R. Moors, K. Spee, S. Plöger, and R. Kruijs, "Progress in EUV optics lifetime expectations," *Microelectron. Eng.* **73-74**, 16–22 (2004).
- H. Meiling, B. Mertens, F. Stietz, M. Wedowski, R. Klein, R. Kurt, E. Louis, and A. Yakshin, "Prevention of MoSi multilayer reflection loss in EUVL tools," *Proc. SPIE* **4506**, 93–104 (2001).
- K. Boller, R.-P. Haelbich, H. Hogrefe, W. Jark, and C. Kunz, "Investigation of carbon contamination of mirror surfaces exposed to synchrotron radiation," *Nucl. Instrum. Methods Phys. Res.* **208**, 273–279 (1983).
- T. Engel, "The interaction of molecular and atomic oxygen with Si(100) and Si(111)," *Surf. Sci. Rep.* **18**, 91–144 (1993).
- G. Y. McDaniel, S. T. Fenstermaker, D. E. Walker, Jr., W. V. Lampert, S. M. Mukhopadhyay, and P. H. Holloway, "Electron-stimulated oxidation of silicon carbide," *Surf. Sci.* **445**, 159–166 (2000).
- T. Miyake, S. Soeki, H. Kato, A. Namiki, H. Kamba, and T. Suzuki, "Molecular-beam study of sticking of oxygen on Si(100)," *Phys. Rev. B* **42**, 11801–11807 (1990).
- R. A. Roseberg and D. C. Mancini, "Deposition of carbon on gold using synchrotron radiation," *Nucl. Instrum. Methods Phys. Res. A* **291**, 101–106 (1990).
- T. Koide, S. Sato, T. Shidara, M. Niwano, M. Yanagihara, A. Yamada, A. Fujimori, A. Mikuni, H. Kato, and T. Miyahara, "Investigation of carbon contamination of synchrotron radiation mirrors," *Nucl. Instrum. Methods Phys. Res. A* **246**, 215–218 (1986).
- M. E. Malinowski, P. Grunow, C. Steinhaus, W. M. Clift, and L. E. Klebanoff, "Use of molecular oxygen to reduce EUV-induced carbon contamination of optics," *Proc. SPIE* **4343**, 347–356 (2001).
- G. Kyriakou, D. J. Davis, R. B. Grant, D. J. Watson, A. Keen, M. S. Tikhov, and R. M. Lambert, "Electron impact-assisted carbon film growth on Ru(0001): implications for next-generation EUV lithography," *J. Phys. Chem. C* **111**, 4491–4494 (2007).
- C. Tarrío and S. Grantham, "Synchrotron beamline for extreme-ultraviolet multilayer mirror endurance testing," *Rev. Sci. Instrum.* **76**, 056101 (2005).
- F. Dong, S. Heinbuch, J. J. Rocca, and E. R. Bernstein, "Dynamics and fragmentation of van der Waals clusters:  $(\text{H}_2\text{O})_n$ ,  $(\text{CH}_3\text{OH})_n$ , and  $(\text{NH}_3)_n$  upon ionization by a 26.5 eV soft x-ray laser," *J. Chem. Phys.* **124**, 224319 (2006).
- S. Heinbuch, F. Dong, J. J. Rocca, and E. R. Bernstein, "Single photon ionization of van der Waals clusters with a soft x-ray laser:  $(\text{CO}_2)_n$  and  $(\text{CO}_2)_n(\text{H}_2\text{O})_m$ ," *J. Chem. Phys.* **125**, 154316 (2006).
- F. Dong, S. Heinbuch, J. J. Rocca, and E. R. Bernstein, "Single photon ionization of van der Waals clusters with a soft x-ray laser:  $(\text{SO}_2)_n$  and  $(\text{SO}_2)_n(\text{H}_2\text{O})_m$ ," *J. Chem. Phys.* **125**, 154317 (2006).
- F. Dong, S. Heinbuch, J. J. Rocca, and E. R. Bernstein, "Formation and distribution of neutral vanadium, niobium, and tantalum oxide clusters: single photon ionization at 26.5 eV," *J. Chem. Phys.* **125**, 164318 (2006).
- S. Heinbuch, F. Dong, J. J. Rocca, and E. R. Bernstein, "Single photon ionization of hydrogen bonded clusters with a soft x-ray laser:  $(\text{HCOOH})_x$  and  $(\text{HCOOH})_y(\text{H}_2\text{O})_z$ ," *J. Chem. Phys.* **126**, 244301 (2007).
- F. Dong, S. Heinbuch, Y. Xie, J. J. Rocca, Z. Wang, K. Deng, S. He, and E. R. Bernstein, "Experimental and theoretical study of the reactions between neutral vanadium oxide clusters and ethane, ethylene, and acetylene," *J. Am. Chem. Soc.* **130**, 1932–1943 (2008).
- S. Heinbuch, M. Grisham, D. Martz, and J. J. Rocca, "Demonstration of a desk-top size high repetition rate soft x-ray laser," *Opt. Express* **13**, 4050–4055 (2005).
- S. Heinbuch, M. Grisham, D. Martz, F. Dong, E. R. Bernstein, and J. J. Rocca, "Desk-top size high repetition rate 46.9 nm capillary discharge laser as photoionization source for photochemistry applications," *Proc. SPIE* **5919**, 591907 (2005).
- M. E. Geusic, M. D. Morse, S. C. O'Brien, and R. E. Smalley, "Surface reactions of metal clusters I: The fast flow cluster reactor," *Rev. Sci. Instrum.* **56**, 2123–2130 (1985).
- Y. Matsuda and E. R. Bernstein, "On the titanium oxide neutral cluster distribution in the gas phase: detection through 118 nm single-photon and 193 nm multiphoton ionization," *J. Phys. Chem. A* **109**, 314–319 (2005).
- T. E. Madey, N. S. Faradzhev, B. V. Yakshinskiy, and N. V. Edwards, "Surface phenomena related to mirror degradation in extreme ultraviolet (EUV) lithography," *Appl. Surf. Sci.* **253**, 1691–1708 (2006).
- Z. Luo, H. Cai, X. Ren, J. Liu, W. Hong, and P. Zhang, "Hydrophilicity of titanium oxide coatings with the addition of silica," *Mater. Sci. Eng., B* **138**, 151–156 (2007).
- M. Ritala, M. Leskelä, L. Niinistö, T. Prohaska, G. Friedbacher, and M. Grasserbauer, "Development of crystallinity and morphology in hafnium dioxide thin films grown by atomic layer epitaxy," *Thin Solid Films* **250**, 72–80 (1994).
- M. Ritala and M. Leskelä, "Zirconium dioxide thin films deposited by ALE using zirconium tetrachloride as precursor," *Appl. Surf. Sci.* **75**, 333–340 (1994).
- M. Atik and M. A. Aegerter, "Corrosion resistant sol-gel  $\text{ZrO}_2$  coatings on stainless steel," *J. Non-Cryst. Solids* **147/148**, 813–819 (1992).